

Transformer core modeling for magnetizing inrush current investigation.

A. Yahiou^a, A. Bayadi^b

^aDepartment of Electrical Engineering, Setif-I- University, Algeria

Abstract

The inrush currents generated during an energization of power transformer can reach very high values and may cause many problems in power system. This magnetizing inrush current which occurs at the time of energization of a transformer is due to temporary overfluxing in the transformer core. Its magnitude mainly depends on switching parameters such as the resistance of the primary winding and the point-on-voltage wave (switching angle). This paper describes a system for measuring the inrush current which is composed principally of an acquisition card (EAGLE), and LabVIEW code. The system is also capable of presetting various combinations of switching parameters for the energization of a 2 kVA transformer via an electronic card. Moreover, an algorithm for calculating the saturation curve is presented taking the iron core reactive losses into account, thereby producing a nonlinear inductance. This curve is used to simulate the magnetizing inrush current using the ATP-EMTP software.

Keywords: Inrush current measurement, transformer, Core nonlinearities, Modelling, ATP-EMTP Simulation.

Nomenclature

ATP	Alternative Transients Program		
EMTP	ElectroMagnetic Transient Program		
B	: Flux density.	R	: Resistance.
i_l	: Magnetizing current.	S_k	: Apparent losses
I_{rms}	: rms current.	V_k	: Peak voltage.
L	: Inductance.	V_{rms}	: rms voltage.
N	: Number of segments.	λ	: Linkage flux.
P_k	: Real losses.	λ_r	: Residual flux.
Q_k	: Reactive losses.	α_j	: Break points

1. Introduction

Magnetizing inrush current in the transformers results from any abrupt changes of the magnetizing voltage. This current in transformer may be caused by energizing an unloaded transformer. Because the amplitude of inrush current can be as high as a short-circuit current [1], a detailed analysis of the magnetizing inrush current under various conditions is necessary

for the concerns of a protective system for the transformers. In this regard, some numerical and analytical methods have been proposed in the literature.

Bertagnoli proposes a relatively simple equation based on a sustained exponential decay of the inrush current [2]. The analytical formula proposed by Specht is somewhat more accurate as the decay of the dc component of the flux (BR) is considered only during saturation ($B > B_S$) [3]. Holcomb proposes an improved analytical equation [4]. We find an improved design method for a novel transformer inrush current reduction scheme in [5]. The used scheme energizes each phase of a transformer in sequence and uses a neutral resistor to limit the inrush current. A transformer model for inrush current simulation based on separate magnetic and electric equivalent circuits is discussed in [6].

Some methods have been used to convert the $(V_{rms} - I_{rms})$ curve to (flux — peak current) curve [7, 8].

In this paper, first, a method to calculate the saturation curve is presented taking the iron core reactive losses into account, thereby producing a nonlinear inductance. It is also shown that the method is applicable for modelling nonlinearities of power transformers. Then, the system for measuring the inrush current is described. The system is also capable of presetting two factors affecting the magnetizing inrush current (resistance and the point- on-voltage wave at the instant of energization). Finally a one-phase transformer is simulated in ATP-EMTP software, the simulation results are compared with the experimental results.

2. Flux and inrush current

As seen from the Fig. 1 (this figure shows the generation of inrush current in a transformer), exceeding flux from the knee point, results in large magnetizing current that in some circumstances can be ten times of the rated current in a transformer.

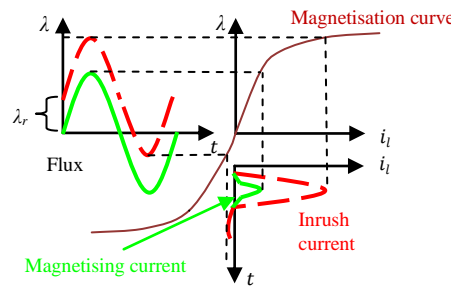


Figure 1. Flux VS magnetizing current.

3. Iron core modelling

Under open circuit test configuration, the equivalent circuit of a power transformer can be reduced to a resistance R_m in parallel with an inductance L_m [9], as shown in Fig. 2.

The main nonlinear element in the transformer’s model is a ferromagnetic inductance L_m . The inductance L_m is defined by gradient $d\lambda/di_1$ in any point of nonlinear magnetizing curve $\lambda = f(i_1)$.

The piecewise linearized curve is shown in Fig. 3.

For computation, the method requires only $(V_{rms} - I_{rms})$ curves and the no-load losses P_k at fundamental frequency. Then, calculates the reactive power Q_k using:

$$S_k = V_{rmsk} * I_{rmsk}$$

$$Q_k = \sqrt{S_k - P_k} \tag{1}$$

Where:

S_k : Apparent power of the segment k .

$k = 1, 2, 3 \dots N$.

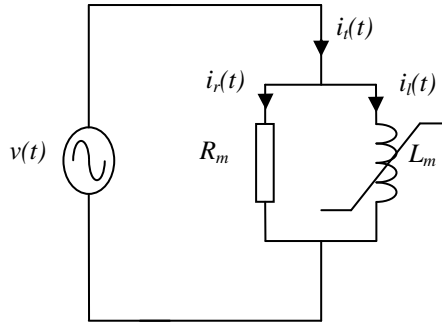


Figure 2. Transformer model for open circuit test.

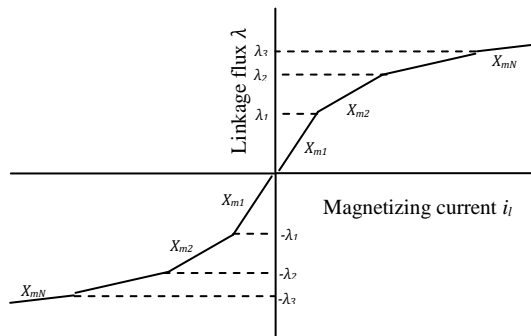


Figure 3. Nonlinear saturation curve.

3.1. Computation of magnetizing curve $\lambda = f(i_l)$

Let us assume that the reactive no-load losses $Q_1, Q_2, Q_3, \dots, Q_n$ are available as a function of the applied voltage $V_{rms1}, V_{rms2}, V_{rms3} \dots V_{rmsn}$, as shown in Fig. 4.

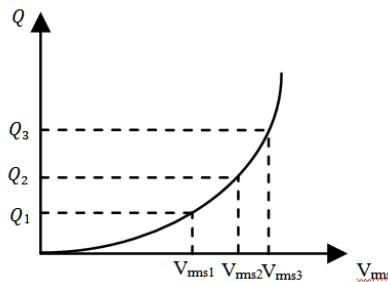


Figure 4. ($Q_k - V_{rms}$) Characteristic.

Because of the symmetry of the $\lambda = f(i_l)$ characteristic with respect to the origin, it is sufficient to observe quart of the cycle, in other word for an angle $\alpha = \pi/2$ (Fig. 5).

In general, $i_1(\alpha)$ can be found for each $v(\alpha)$ through the nonlinear $v = f(i_l)$ characteristic, either graphically as indicated by the dotted lines in Fig. 8. This will give us the curve $i_1(\alpha)$ over quart of a cycle, from which the no-load reactive losses are found:

$$Q = \frac{2}{\pi} \int_0^{\frac{\pi}{2}} v(\alpha) i_l(\alpha) \tag{2}$$

Let us address the reverse problem, i.e., constructing the $\lambda = f(i_l)$ from the given no-load reactive losses.

For $k = 1$ the reactance X_1 is equal:

$$X_1 = \frac{V_{rms1}^2}{Q_1} \tag{3}$$

The current of the first segment is:

$$i_{l1} = \frac{V_{rms1} \sqrt{2}}{X_1} \tag{4}$$

For $k \geq 2$, we must use the reactive power definition of equation (2), with the applied voltage $v(\alpha) = V_k \sin(\alpha)$.

$$Q_k = \frac{2}{\pi} \left[\int_0^{\alpha_1} V_k \sin(\alpha) \left(\frac{V_k \sin(\alpha)}{X_1} \right) d\alpha + \int_{\alpha_1}^{\alpha_2} V_k \sin(\alpha) \left(i_{l1} + \frac{V_k \sin(\alpha) - V_1}{X_2} \right) d\alpha + \dots + \int_{\alpha_{k-1}}^{\frac{\pi}{2}} V_{k-1} \sin(\alpha) \left(i_{lk-1} + \frac{V_k \sin(\alpha) - V_{k-1}}{X_k} \right) d\alpha \right] \tag{5}$$

With V_k is the peak voltage.

$$V_k = V_{rmsk} \times \sqrt{2} \tag{6}$$

The points $\alpha_1, \alpha_2, \dots, \alpha_{k-1}$ in equation (5) are known using:

$$\alpha_j = \sin^{-1} \frac{V_j}{V_k} ; \quad j = 1, 2, \dots, k - 1 \tag{7}$$

The only unknown factor in equation (5) is the slope X_k of last segment during the current calculation of the same slope.

Equation (5) can be rewritten as follows (simplified form):

$$Q_k = c_{lk} + \frac{y_{lk}}{X_k} \tag{8}$$

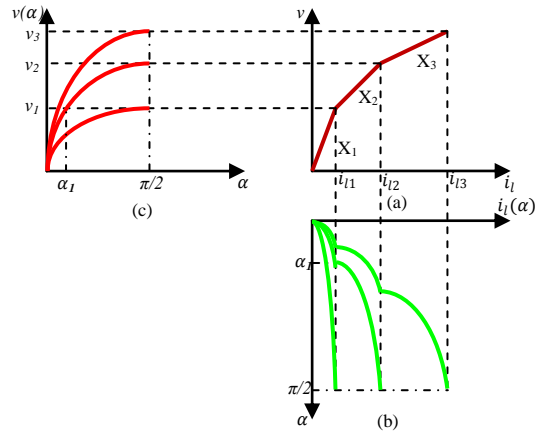


Figure 5. Calculation of the nonlinear inductance.

(a) $v = f(i_l)$ Curve, (b) Output current, (c) Sinusoidal input voltage signal.

The current i_l is obtained by:

$$i_{lk} = i_{lk-1} + \frac{V_k - V_{k-1}}{X_k} \quad (9)$$

The above mentioned procedure stages for calculating the saturation curve are summarized in the following flow chart (Fig. 6).

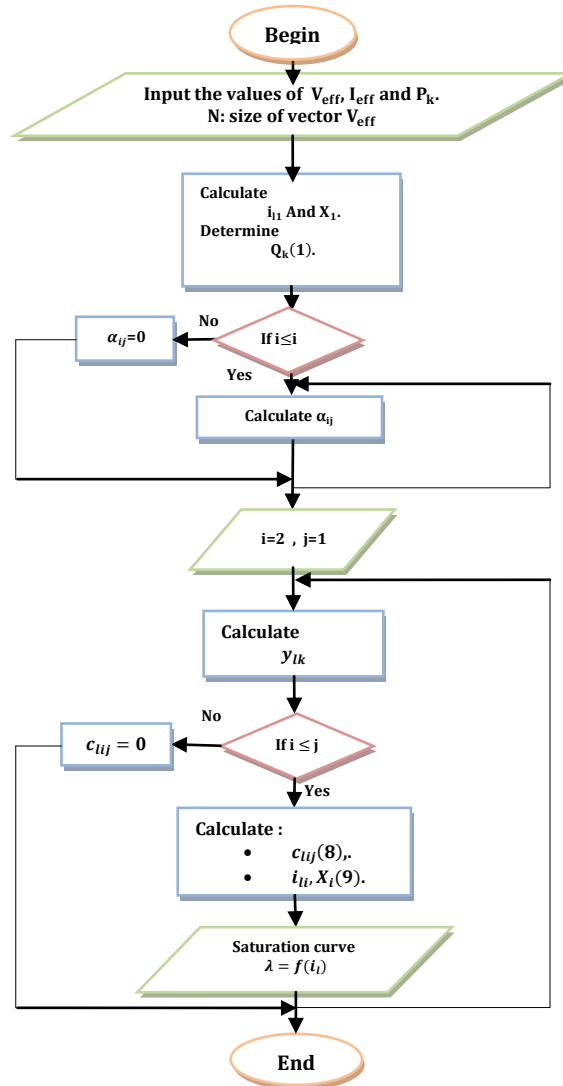


Figure 6. Flow chart to compute $\lambda = f(i_l)$.

No load losses and rms current at 50 Hz were measured for different voltage levels are shown in Table I.

According to Faraday’s law and in case of a sinusoidal applied voltage, it can be written [10].

$$\lambda_k = \frac{V_k}{\omega} \tag{10}$$

The computed points (including core losses) using our approach are shown in table II. The results obtained using the method described in [11] are included for comparison purposes. The obtained $\lambda = f(i_l)$ characteristic is shown in Fig. 7.

It is noted that there is a superposition up to the point (127.0708, 0.6874) because the transformer has an internal capacitance between the coils and between the winding and the ground. Therefore there is a small current i_c in the magnetizing branch of the equivalent circuit.

As can be seen, for the same value of λ , the current i_l calculated using our approach has a value higher than that calculated by [11], which enables us to predict more exact peak inrush current in the simulation (Fig 13).

Table 1. ($V_{rms} - I_{rms}$) Curve point and Corresponding Active Power Losses.

P (W)	I_{rms} (A)	V_{rms} (V)
0	0	0
0.025	0.005	9.900
0.25	0.013	31.3
1.28	0.026	67.2
3.1	0.042	107.9
6.5	0.084	152.7
12	0.217	194.1
17	0.369	220
19	0.408	225.6
20.500	0.435	229.300

Table 2. Calculated Points Of $\lambda = f(i_l)$ curve.

i_l (mA)	i_l [11](mA)	λ (V.s)
0	0	0
6.1030	6.1030	0.0446
13.8743	13.8339	0.1409
23.7278	23.6217	0.3025
45.0400	44.9937	0.4857
127.0708	122.7732	0.6874
431.8758	393.5898	0.8738
766.8098	697.2619	0.9903
838.4082	765.6141	1.0156
886.2378	809.4472	1.0322

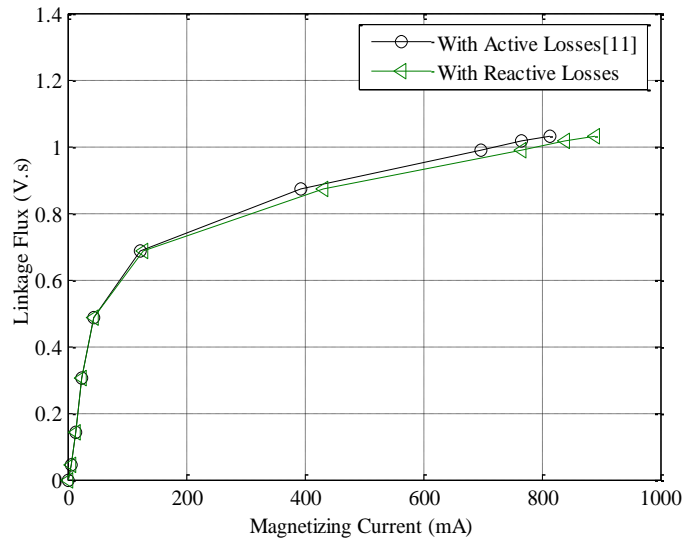


Figure 7. Magnetization (saturation) curve $\lambda = f(i_l)$.

4. Measurement setup of inrush current

One power transformer (2 kVA) has been used for laboratory investigations. This transformer is manufactured by unilab laboratory (Italy). It is unloaded; the high voltage side is connected to voltage supply. The laboratory arrangement with the voltage and current measurement points is shown in Fig. 8. A photo is shown in Fig. 9.

The data acquisition system has been used to record voltages and currents at the high voltage side. A total of fifteen analogue input channels with simultaneous sampling are available. The input voltage can be selected among ± 10 V. The graphical user interface in LabVIEW is shown in Fig. 10.

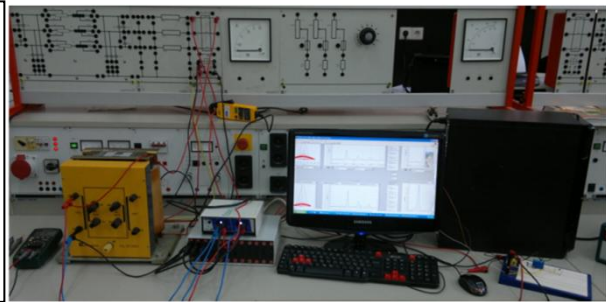
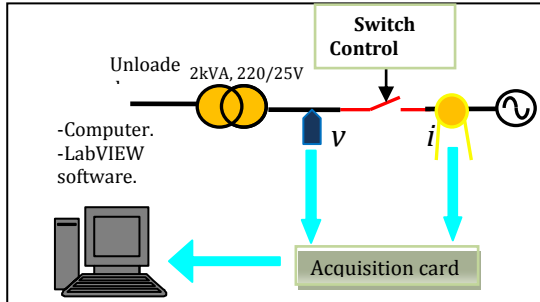


Figure 8. Measurement setup scheme.

Figure 9. Laboratory setup photo.

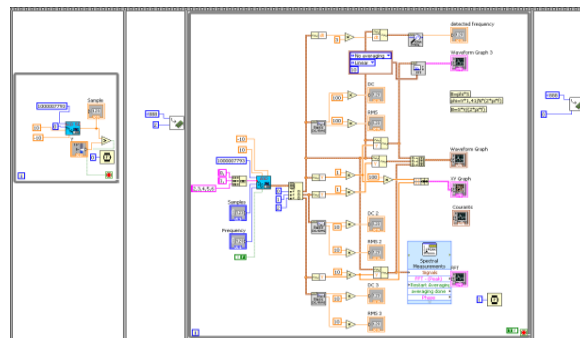
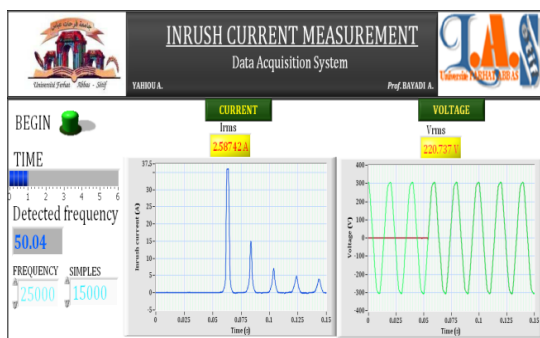


Figure 10. LabVIEW acquisition interface.

Figure 11. LabVIEW acquisition diagram.

5. Measured and simulated inrush current comparison

When a transformer is energized under no load or lightly loaded conditions, inrush current may flow in the primary circuit.

In order to investigate the effects of some parameters of transformer or network on the inrush current, a single-phase transformer (2 kVA, 220/25 V, 9.1/80 A) is selected. The equivalent circuit can be shown in Fig. 12 where R , L , R_m , L_m and R_s are equivalent resistance, leakage inductance of transformer, core losses resistance, magnetizing inductance and source resistance respectively.

Table III presents the parameters obtained according to standards short and open circuit tests.

This circuit is simulated using ATP-EMTP software. The BCTRAN module and external nonlinear inductance type 93 representing the saturation curve have been used in this simulation.

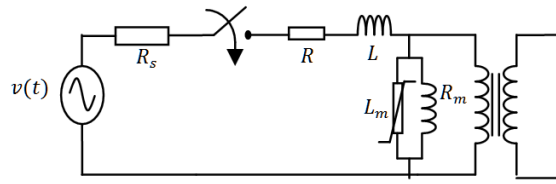


Figure 12. Simulation model of transformer.

Table 3. Transformer parameters.

Parameter	$R(\Omega)$	$L(mH)$	$R_m(\Omega)$
Value	3.48	8.7	2847.1

5.1. Simulation by Using the both Saturation Curves

Fig. 13 shows the peak of the measured and simulated inrush current; in the simulation one introduces the both curves in the magnetizing branch, obtained by the method based on the active losses [11], and the method presented in this paper.

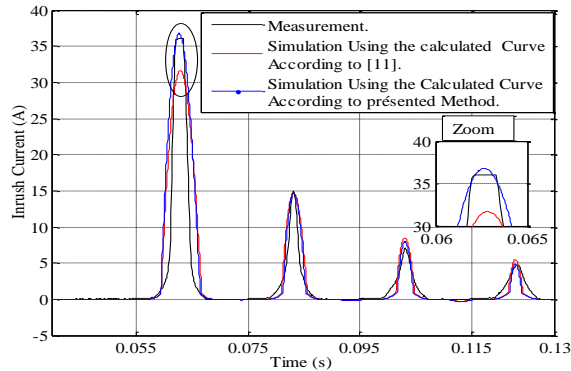


Figure 13. Inrush current comparison.

As shown in above figure; it is clear that the peak of the inrush current obtained with using the calculated curve by taking the iron core reactive losses into account, near to the measured peak. So we have a good prediction of the peak Inrush current in the following application.

5.2. Effects of source resistance (R_s)

In this case, the switching angle (θ) is considered 0° (primary voltage is 0 V). The effects of series resistance have been considered by increasing R_s .

The effect of source resistance on the amplitude of inrush current is presented in Fig. 14.

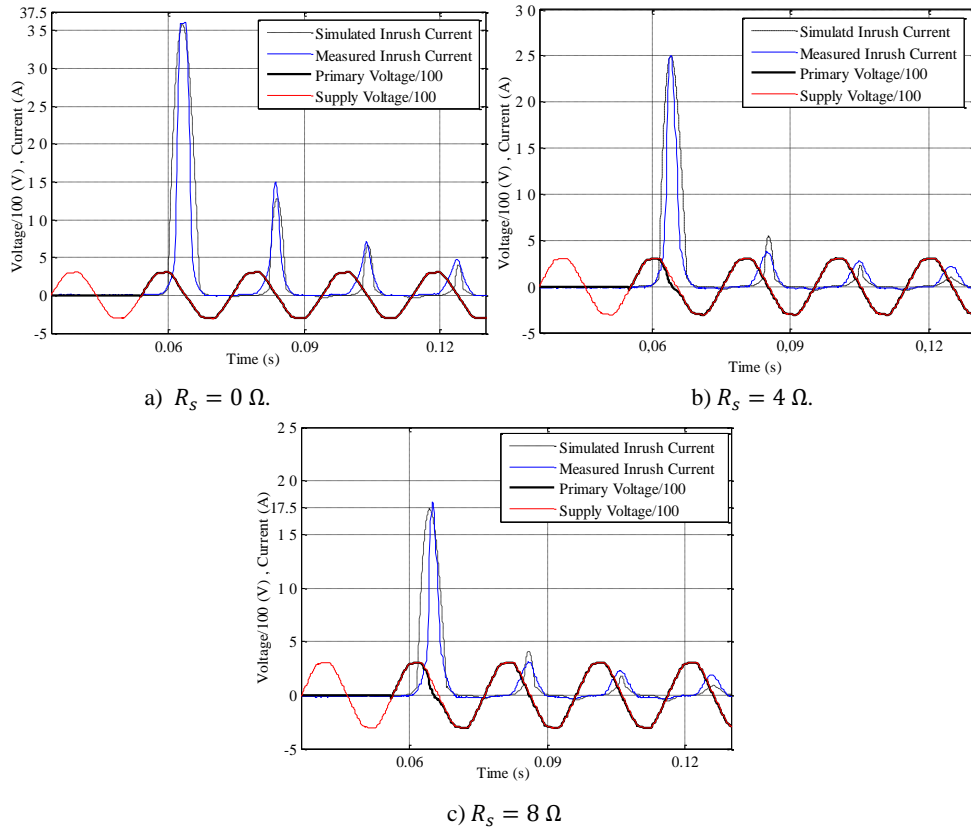


Figure 14. Measured and simulated inrush current for different values of R_s .

As can be seen from Fig 13, increasing source resistance will decrease the amplitude of inrush current. Moreover, it causes faster decay in the amplitude of inrush current. Therefore, it can be said that transformers located closer to the generating plants display higher amount of inrush currents lasting much longer than transformer installed electrically away from generator.

5.3. Effect of the switching angle (Point- On-Voltage)

In this section, the effect of the closing moment of circuit breaker or the point on the voltage wave where the circuit breaker is closed has been investigated. In this case the series resistance is ignored.

The first result was already presented in Fig. 14 a. Fig. 15 presents the first measured and simulated five peaks of inrush current when the applied voltage is equal to 195 V and then to 182 V (i.e. for closing times $t = 0,0492s$ and $t = 0,0501s$ respectively).

It is noted that the highest inrush current amplitude took place when the value of the primary voltage of the transformer is equal to zero. Moreover, the increase in the angle on the voltage wave makes decrease of its amplitude. The energization of the power transformers with a random circuit breaker closing can generate very important amplitude of inrush current. So, it is necessary to control the circuit breaker to choose the optimal moment as a function of the network voltage which allows opening or closing the circuit breaker.

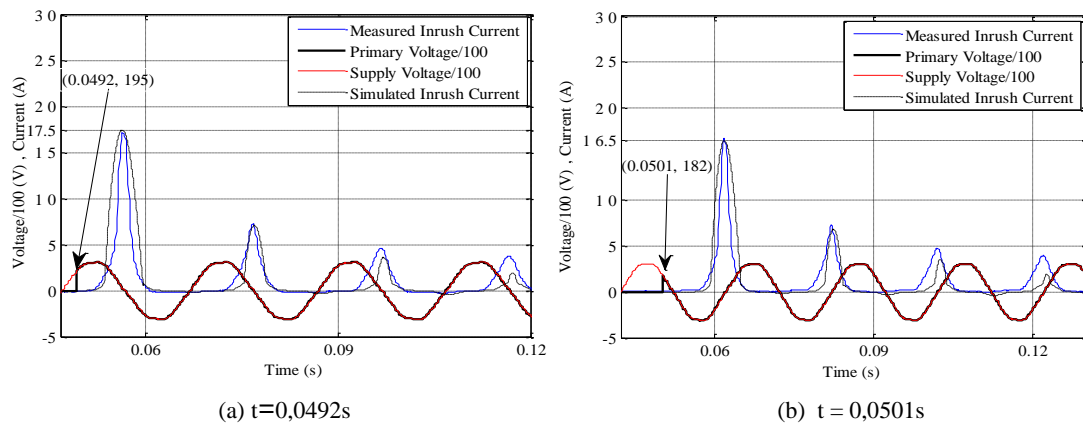


Figure 15. Measured and simulated inrush current for different Point- On-Voltage.

6. Conclusion

In This paper a system for measuring the inrush current which is composed mainly of an acquisition card and LabVIEW code is described. The system is capable of presetting various combinations of switching parameters for the energization of a 2 kVA transformer via an electronic card. Moreover, an algorithm for calculating the saturation curve is presented taking the iron core reactive losses into account, thereby producing a nonlinear inductance. This curve is used to simulate the magnetizing inrush current using the ATP-EMTP software.

The results show that increasing switching angle (the point on the voltage wave) or source resistance will decrease the amplitude of inrush current. Therefore, the transformers located closer to the generating plants display higher amount of inrush currents lasting much longer than transformer installed electrically away from generator.

Moreover, it can be concluded that, for reducing inrush current, an appropriate switching angle by considering residual flux, must be taken into account.

7. References

- [1] Steurer M., Fröhlich K, "The Impact of Inrush Currents on the Mechanical Stress of High Voltage Power Transformer Coils", IEEE Trans. on Power Delivery, Vol.17, No.1, Jan 2002, pp. 155-160.
- [2] G. Bertagnolli, Short-Circuit Duty of Power Transformers, Second Revised Edition. ABB, 1996
- [3] T. R. Specht, "Transformer magnetizing inrush current" , AIEE Trans, Vol. 70, 1951, pp. 323-328
- [4] J. F. Holcomb, "Distribution transformer magnetizing inrush current", Transactions of the American Institute of Electrical Engineers, Part III (Power Apparatus and Systems), Vol. 80, No. 57, Dec. 1961, pp. 697-702
- [5] Sami G. Abdulsalam, and Wilsun X " Analytical Study of Transformer Inrush Current Transients and Its Applications" , IPST'05 - International Conference on Power Systems Transients, Montreal, Canada June 19-23, 2005, No. 140
- [6] N. Chiesa, B. A. Mork, and H. K. Høidalen, " Transformer Model for Inrush Current Calculations: Simulations, Measurements and Sensitivity Analysis", IEEE Trans on Power Delivery, Vol. 25, No. 4, Oct 2010, pp. 2599-2608

- [7] A. Tokic, I. Uglesic, et F. Jakl, " An algorithm for calculations of low frequency transformer transients", IPST'03 - International Conference on Power Systems Transients, , New Orleans, Louisiana, USA, Sep. 2003 No. 9a-2
- [8] W.Wiechowski, B.Bak-Jensen, C. Leth Bak, J. Lykkegaard " Harmonic Domain Modelling of Transformer Core Nonlinearities Using the DIgSILENT PowerFactory Software" ,Electrical Power Quality and Utilisation, Journal, Vol. XIV, No. 1, 2008
- [9] Joydeep Mitra "Advanced transformer modelling for transients simulation" Department of Electrical and Computer Engineering, North Dakota state University, Fargo, North Dakota 58105, July 21, 2003
- [10] Arrillaga J., Watson N.R.: "Power System Harmonics". John Willey & Sons, London, 2003, p. 62–64
- [11] Neves L.A.N., Dommel H.W.: "On Modelling Iron Core Nonlinearities". IEEE Trans on Power Systems, Vol. 8, No. 2, May 1993, pp. 417–425